MABS
2016, VOL. 8, NO. 8, 1525–1535
http://dx.doi.org/10.1080/19420862.2016.1231277

Taylor & Francis
Taylor & Francis Group

REPORT

OPEN ACCESS

Oxidation in the complementarity-determining regions differentially influences the properties of therapeutic antibodies

Tetyana Dashivets[a,b], Jan Stracke[c], Stefan Dengl[a], Alexander Knaupp[a], Jan Pollmann[d], Johannes Buchner[b], and Tilman Schlothauer[a]

[a]Roche Pharma Research and Early Development (pRED), Large Molecule Research, Roche Innovation Center Munich, Germany; [b]Center for Integrated Protein Science Munich, Department Chemie, Technische Universität München, Garching, Germany; [c]Early-Stage Pharmaceutical Development & GLP Supplies, F. Hoffmann-La Roche Ltd Pharmaceutical Development & Supplies PTD Biologics Europe, Basel, Switzerland; [d]Roche Pharma Biotech Penzberg, Germany

ABSTRACT

Therapeutic antibodies can undergo a variety of chemical modification reactions in vitro. Depending on the site of modification, either antigen binding or Fc-mediated functions can be affected. Oxidation of tryptophan residues is one of the post-translational modifications leading to altered antibody functionality. In this study, we examined the structural and functional properties of a therapeutic antibody construct and 2 affinity matured variants thereof. Two of the 3 antibodies carry an oxidation-prone tryptophan residue in the complementarity-determining region of the V_L domain. We demonstrate the differences in the stability and bioactivity of the 3 antibodies, and reveal differential degradation pathways for the antibodies susceptible to oxidation.

Abbreviations: CD, circular dichroism; CDR, complementarity-determining region; CHO, Chinese hamster ovary; Fab, fragment antigen binding; Fc, fragment crystallizable; HPLC, high performance liquid chromatography; LCMS, liquid chromatography mass spectrometry; mAb, monoclonal antibody; PTM, post-translational modifications; SEC, size-exclusion chromatography; SPR, surface plasmon resonance

ARTICLE HISTORY
Received 5 February 2016
Revised 11 August 2016
Accepted 28 August 2016

KEYWORDS
Deamidation; monoclonal antibody; oxidation; posttranslational modifications; succinimide; stability; target binding

Introduction

Recombinant monoclonal antibodies (mAbs) are now commonly used for the treatment of cancer and autoimmune diseases.[1] These bifunctional molecules are able to specifically target and bind their antigen through the variable domains in the Fab part of the antibody. In addition, the Fc region of the antibody interacts with various Fc-receptors, triggering effector functions and defining longevity of the antibody in serum.[2,3]

During development and manufacturing, mAbs can be exposed to different stress factors, e.g., temperature and pH changes, elevated temperature, freezing, thawing, mechanical stress, light exposure, that can potentially result in modifications of the protein, and lead to their degradation.[4-7] To date, various antibody modifications have been reported and described, e.g., oxidation, deamidation, succinimide formation, isomerization; C-terminal lysine cleavage, C-terminal lysine/glycine amidation. As a result, depending on the modification site, either antigen binding or Fc-mediated functions might be impeded, leading to changes in the clinical performance of the therapeutic antibodies.[6-10]

Protein oxidation can be triggered during the production process by metal ions and peroxides that are present as impurities, or it can be caused by light. Methionine is commonly affected; however oxidation of several other amino acids like tryptophan, cysteine, lysine and histidine has been observed.[8,11-14] Oxidation of Met or Trp residues in the Fc was reported for several antibodies. These antibodies were shown to have impaired Fc-mediated activity, e.g., decreased interaction with protein A and G, FcRn and FcγRs.[8,10,15-20] There are fewer studies on oxidation of Met/Trp residue in the antibody complementarity-determining regions (CDRs). Nevertheless, it has been demonstrated for several antibodies that such modifications reduced or even abolished target binding of these molecules.[13,21-23]

Asparagine deamidation and aspartate isomerization are modifications that frequently occur under mild stress conditions. Asparagine residues can form succinimide intermediates, which upon hydrolysis yield a mixture of aspartate and isoaspartate at an approximate ratio of 1:3. It was demonstrated that the deamidation rate was dependent on the temperature and buffer composition, as well as buffer pH.[24-26] Furthermore, C-terminal amino acids near the critical Asn were reported to have an influence on its deamidation propensity. For instance, glycine, serine and histidine residues were observed to favor succinimide formation.[9,27-30] Deamidation and aspartate isomerization were also demonstrated to be critical for antibody activity, especially for the target binding.[9,31-34]

Along with decreased activity, such modifications might lead to other unwanted effects, including a decrease in stability and an increase in immunogenicity. Thus, it is important to

CONTACT Tilman Schlothauer tilman.schlothauer@roche.com
Supplemental data for this article can be accessed on the publisher's website.

examine the effect of mAb modifications on the structural and functional properties of the antibody.

Oxidation of mAbs can be achieved by treatment with H_2O_2, tBHP, 2,2′-azobis(2-amidinopropane (AAPH), irradiation or ozone.[8,11,13,17,35,36] The modified antibody species exhibit differential biophysical properties (charge, hydrophobicity or stability), which enables their separation from the main unmodified antibody fraction by different chromatographic methods. This allows the identification of the modified residues by mass spectrometry (MS) analysis.[13,23,31,37-43] Replacement of the identified modification-prone residue could solve the problem, but one should keep in mind that the mutation might affect other properties, including a loss of function.[44,45]

In this work, we present a case study on the bispecific XGFR antibody[46] comprising a Fab for monovalent binding of epidermal growth factor receptor (EGFR) and a single chain Fab specific for human insulin-like growth factor 1 receptor (IGF-1R) (Fig. 1). We focused on the IGF-1R binding CDRs of parental AK18 (R1507) human IgG1 mAb[47,48] and 2 of its affinity-matured variants. The rest of the antibody scaffold was identical, and was regarded as not relevant for the direct comparison of the degradation pathway.

The parental AK18 antibody and one of the variants carry modification-prone amino acids in their CDRs. Here, we report the effect of stress conditions on the structure, stability and activity of the addressed mAbs, and demonstrate a differential influence of Trp oxidation on the properties of the antibodies studied. As the antibodies examined in this work demonstrate an identical composition except for the variable region of the light chain, respective single V_L domains were analyzed with regard to their structural properties and stability, followed by the structural and functional analysis of the entire variable region (single-chain fragment variable, scFv) (Fig. 1).

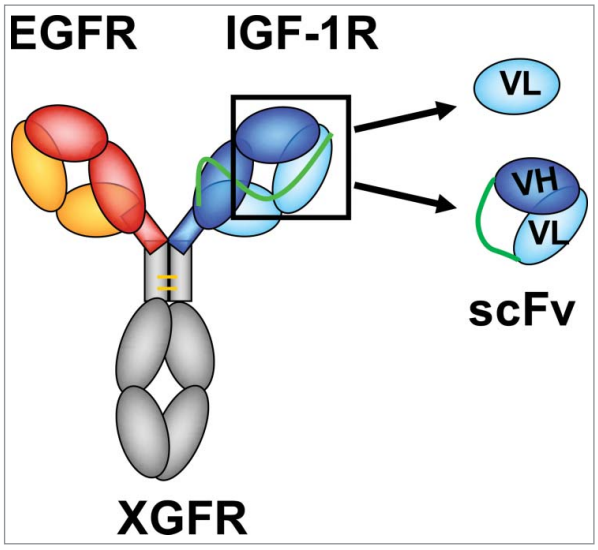

Figure 1. Antibody formats used in the study. XGFR is a bispecific antibody consisting of EGFR-binding Fab shown in red and yellow and IGF-1R-binding single chain Fab in dark blue and light blue. In addition to full-length antibody, VL (variable domain of light chain) and scFv (single chain fragment variable) of the IGF-1R binding region were analyzed in this study.

Results

Oxidation of AK18

To increase its therapeutic efficacy, the IGF-1R binding region of XGFR was subjected to affinity maturation by random mutagenesis of CDRs and phage display. As a result, 2 antibody variants with a 10-fold higher IGF-1R affinity, compared to the parental mAb, were identified. In this work, we analyzed 3 XGFR variants, which differ only in the composition of IGF-1R binding CDRs of V_L, within the respective scFabs, as summarized in Table 1. These XGFR antibody variants will be referred to as AK18, F15B5 and L31D11.[46]

To compare their stabilities and aggregation propensities, we performed dynamic light scattering measurements at increasing temperatures. The parental AK18 XGFR and F13B5 started to aggregate at 55°C. In contrast, antibody variant L31D11 was already aggregated at 45°C. To determine the melting temperature (Tm) of the test antibodies, we detected changes in their intrinsic fluorescence upon temperature increase, which reflects the conformational changes upon unfolding. In addition, light scattering at 266 nm enables monitoring of the protein aggregation.[49,50] AK18 and F13B5 demonstrated Tms of 61°C and 59°C, respectively, whereas L31D11 was less stable (Tm 51°C). The trend obtained by this method is thus equivalent to that obtained by DLS (Table 2).

Next, the 3 antibodies were exposed to various forced stress conditions, such as freeze-thawing, prolonged incubation at 40°C or treatment with 1 mM AAPH dihydrochloride to promote oxidation. Subsequently, the aggregation propensity, integrity, stability and functionality of the stress-exposed mAbs with reference to the unstressed antibody samples were determined.

Size-exclusion chromatography (SEC) was employed to address aggregate formation or fragmentation of the stress-exposed antibody samples. The SEC analysis revealed that freeze/thawing did not affect the tested antibodies, as no loss of the monomeric IgG fraction could be detected (Fig. 2). In contrast, incubation at elevated temperature resulted in the prominent aggregation of the L31D11 antibody variant, whereas AK18 and F13B5 remained mostly unaffected. For oxidation stress, slightly increased formation of high molecular weight species (HMW) was observed solely for the parental AK18, the 2 variants retained their monomeric state (Fig. 2). Low molecular weight species (LMW), which might occur as a result of protein degradation, were not detected for any of the antibody variants under the applied stress conditions.

Table 1. Composition of CDRs of XGFR antibody variants.

Antibody	V_L CDR1	V_L CDR2	V_L CDR3	pI
AK18	ASQSVSSYLAWY	IYDASKRA	QQRSKWPPWTFG	9.4
L31D11	ASRSVYSSLAWY	IYKASSRA	QQRSKWPPWTFG	9.4
F13B5	ASQSVSSYLAWY	IYQASKRA	QQRSKYPPWTFG	9.4

Table 2. The aggregation and melting temperatures of the 3 XGFR variants.

	Tm IF	Tagg IF	Tagg DLS
AK18	~58°C	~58°C	~58°C
L31D11	~46°C	~46°C	~45°C
F13B5	~56°C	~56°C	~55°C

IF intrinsic fluorescence, DLS dynamic light scattering.

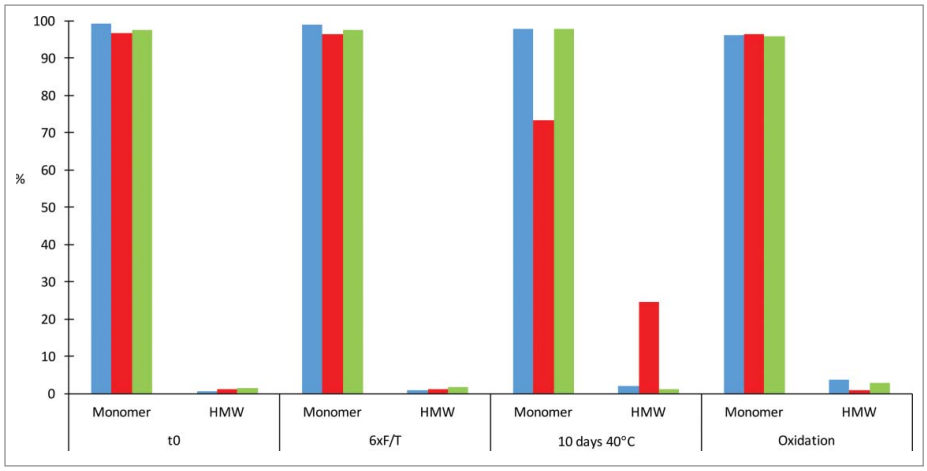

Figure 2. SEC analysis of stress exposed XGFR antibody variants. The monomer and high molecular weight species content of the samples is shown for AK18 in blue, L31D11 in red and F13B5 in green. The unstressed antibody samples (t0) were compared to samples subjected to multiple freeze/thawing (6xF/T), incubation at 40°C for 10 d (10d 40°C) and oxidation (ox). SEC analysis was carried out in 200 mM K-Phosphate, 250 mM KCL, pH 7.0.

To determine the effect of the forced stress conditions on the antibody functionality, surface plasmon resonance (SPR) was applied. The stress-exposed antibody samples were captured by protein A, immobilized on the chip surface, and then IGF-1R was injected as analyte. First, the interaction of IGF-1R with the stressed antibodies was assessed in the non-kinetic comparative manner. Here, the antibody and the IGF-1R target were applied at a fixed concentration, and differences at the end of the association phase were used for the relative difference evaluation. The binding activity of the respective unstressed antibody sample was applied as a reference.

Comparative analysis of antibody-target interactions revealed that freeze/thawing did not have a negative effect on antibody activity of any of the tested samples. Incubation at elevated temperatures also did not affect target binding of F13B5, but resulted in slightly decreased binding for L31D11 and AK18 compared to the unstressed antibodies. However, a decrease of ~30% was detected for the AK18 antibody after the oxidative stress. Binding of oxidized L31D11 and F13B5 to IGF-1R remained mostly unaffected. To examine the stability of the interaction of the stressed mAbs with their target, the dissociation behavior of the samples 360 sec after the injection stop was compared. The interaction of the stress-exposed L31D11 and F13B5 antibodies with IGF-1R was stable and comparable to that of the unstressed antibodies. Thermally treated and oxidized AK18 showed higher stability of binding, indicating presence of the aggregates (Fig. 3).

For the kinetic analysis of the antibody-antigen interactions, the test antibodies were captured again by protein A on the chip surface, and then IGF-1R was injected as analyte at different concentrations. For the unstressed antibody samples, as well as oxidized F13B5 and L31D11, a classical 1:1 interaction evaluation algorithm was applied to determine the binding constants (Table 3). Oxidation of AK18 resulted in impaired antigen interaction, and evaluation of the resulting signal was not possible. From the kinetic evaluation of oxidized AK18, we observed that at a low antibody capture level mainly the dissociation of IGF-1R was impaired (see Fig. S1A and 1B). At 5-fold higher antibody capture levels, as applied for the active binding determination, only 30% reduction was observed, indicating that this setup is less sensitive to off-rate impairing binding defects. Due to the setup, it is possible that avidity compensates for the defect in the oxidized CDRs and 70% of the oxidized AK18 are still able to bind IGF-1R receptor, which is known for dimerization (see Fig. S2).

The severe target binding defects monitored for the AK18 variant after oxidation, suggested the presence of oxidation-sensitive amino acid residues in the CDRs of its light chain

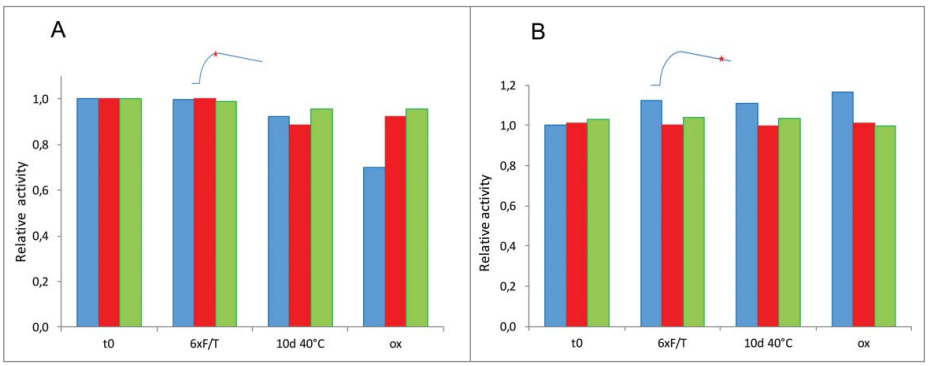

Figure 3. SPR analysis of the target binding activities of the stressed XGFR antibody samples (AK18 in blue, L31D11 in red and F13B5 in green. Activities of the unstressed antibodies (t0) were compared to those of mAb samples subjected to multiple freeze/thawing (6xF/T), incubation at 40°C for 10 d (10d 40°C) and oxidation (ox). (A) IGF-1R binding activities measured 170 sec after injection. (B) Stability of binding activities was measured 360 s after the injection stop.

Table 3. Kinetic assessments of the target binding of IGF-1R binding of XGFR variants.

mAb	ka (1/Ms)	ka ox (1/Ms)	k_d (1/s)	k_d ox (1/s)	K_D [M]	K_D ox [M]
F13B5	7.551E+4	3.846E+4	6.604E-5	2.625E-4	8.613E-10	6.825E-9
L31D11	7.276E+4	4.594E+4	1.205E-4	0.001081	1.656E-9	2.354E-8
AK18	3.951E+4	n.d.	0.002062	n.d.	5.219E-8	n.d.

ka, association constant; k_d, dissociation constant; K_D, binding constant, ox, after oxidation.

since the heavy chain is identical for all 3 mAbs. Analysis of amino acid sequences of the test antibodies by the hot spot predictor software JaHu[28] discovered no Asp/Asn degradation hotspots for any of the 3 antibodies. However, it predicted that the tryptophan residue at position 94 in the CDR3 of the light chain of AK18 and L31D11 variants might be potentially susceptible to oxidation. In addition, *in silico* modeling of the antigen binding pocket confirmed that this Trp is extremely solvent exposed, which increases the probability of an oxidation event (Fig. 4). The F13B5 variant carries in this position a tyrosine residue instead of the critical Trp, and in this case oxidation did not influence antigen binding.

To address this matter, and to investigate whether the identified Trp-residues are indeed oxidized, the respectively stressed antibody samples were analyzed by ESI MS. The obtained peptide mapping results demonstrated that the major structural modifications were caused by oxidative stress in L31D11 and AK18. In L31D11, 93.7% of the solvent exposed Trp94 was oxidized. AK18 showed 42.7% oxidation of the respective residue (Table 4).

In summary, comparative analysis of the stability, integrity and activity of the 3 antibody variants delivered very different and surprising results. In terms of thermal stability, the L31D11 variant demonstrated the lowest melting temperature and aggregated first. The exposure of the 3 mAbs to different stress conditions revealed no influence of multiple freezing/thawing on any of the tested proteins. Incubation of the antibody samples at elevated temperature resulted in the measurable aggregation of L31D11; AK18 and F13B5 stayed intact. Formation of HMW species upon oxidative stress was observed only for AK18 mAb. Analysis of the functionality of the stress-subjected antibodies revealed that any of the applied stress conditions did not have a prominent effect on the target binding for F13B5. In contrast, incubation at elevated temperatures resulted in a slight drop in binding activity of AK18 and L31D11. Moreover, for AK18, target binding was almost abolished after oxidation, in the direct comparative kinetic evaluation.

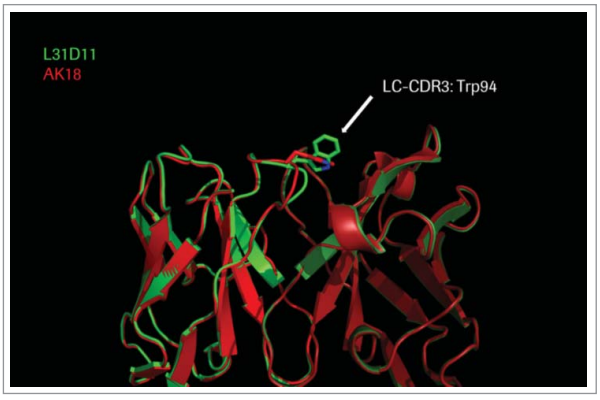

Figure 4. In silico analysis of AK18 (red) an L31D11 (green) antigen binding regions. Models of antigen binding regions revealed strongly exposed tryptophan at position 94.

Characterization of V_L domains

Analysis of the structural and functional properties of the test antibodies revealed major differences in stability, aggregation behavior and target binding. The three antibodies differ just by their V_L domains, whereas the remaining structural units are identical for all three. Thus, we set out to systematically examine the respective V_L domains of the AK18 and its variants, and compare their structure and stability.

The V_L domains of AK18, F13B5 and L31D11 were produced in *Escherichia coli* as inclusion bodies (IBs), refolded to their native state and purified to homogeneity. The V_L domain in the context of the whole antibody is a part of heterodimer and was reported to form homodimers in its isolated form.[51] To investigate the quaternary structure of the isolated, V_L domains, we carried out HPLC SEC (Fig. 5). The SEC analysis of all obtained antibody domains demonstrated the presence of a single protein fraction with an elution time corresponding to a mass of ca. 12 kDa, which is a mass of the monomeric protein species. Aggregates or degradation products could not be detected for either of the tested protein samples. Thus, the obtained V_L domains are monomers.

Far-ultraviolet (UV) circular dichroism (CD) spectroscopy demonstrated that the refolding process yielded correctly folded proteins. Analysis of V_L domains gave spectra, indicative of the ß-sheet protein with a signal minimum at 218 nm, and a low overall intensity (Fig. 6A). However, the obtained spectra were not identical, indicating differences in the secondary structure of the examined VLs. Differences were also observed in the near UV-CD spectra, which represents the tertiary structure of the proteins, and especially the environment of the aromatic amino acids (Fig. 6B).

Next, far-UV CD spectroscopy was employed to assess the thermal stability of the V_L domains of AK18 and its variants. Here, temperature-induced changes in the secondary structure of the V_L domains were monitored at 218 nm (Fig. 7). The midpoint of the transition determined for AK18 and F13B5 was at 57°C, while L31D11 exhibited lower thermal stability (transition midpoint at 48°C). Interestingly, thermal stability of the complete L31D11 antibody was also lower compared to the remaining 2 mAb variants.

The analysis of isolated V_L domains enabled insight into the differences in their structure and stability. The contribution of the CDRs of V_H is crucial for the formation of antigen binding. Consequently, the isolated V_L -domains of all 3 antibodies failed to bind the target. Thus, we combined the V_H and V_L domains via a GS linker to produce scFvs (described in the experimental section) and addressed their functional and structural properties.

Structural and functional properties of the scFvs

scFv of AK18, L31D11 and F13B5 were expressed in Chinese hamster ovary (CHO) cells in their native form and purified to

Table 4. Analysis of Tryptophan oxidation of XGFRvariants.

	% modified peptide								
AA	AK18	AK18 40°C 10d	AK18 oxidized	L31D11	L31D11 40°C 10d	L31D11 oxidized	F13B5	F13B5 40°C 10d	F13B5 Oxidized
Trp 94	0.6	0.9	42.7	1.0	1.6	93.7	n/a	n/a	n/a

AA – amino acid.

heterogeneity. The SEC analysis revealed that all 3 purified scFv constructs were monomers.

To induce oxidation, scFvs were treated with AAPH, and incubated for 24 h at 40°C, as described in the experimental section. Thermal unfolding of the scFvs was again monitored by changes in the intrinsic fluorescence upon temperature increase. Additionally, light scattering was used to monitor the aggregation behavior of the scFvs. The melting and aggregation temperatures of the 3 scFvs are summarized in Table 5.

In line with the results obtained for the intact antibody and V_L domain, L31D11 demonstrated the lowest stability, with a melting temperature of 43°C and aggregation temperature of 41°C. Analysis of the oxidized L31D11 was not possible because, due to its low thermal stability, the L31D11 samples did not survive the oxidation that occurred during the incubation period. The AK18 scFv exhibited the highest melting/aggregation temperatures (52°C and 50°C, respectively); however, after the oxidation stress its aggregation temperature was decreased by 4°C. The F13B5 scFv variant appeared to be more stable than L31D11, but less stable than AK18; its stability was mostly unaffected by oxidation (Table 5).

When the aggregation propensity of the oxidation-exposed scFvs was assessed by SEC, oxidation of L31D11 resulted in a complete precipitation of the sample. The analysis of the remaining 2 variants did not reveal any major loss of the monomer; however, oxidized AK18scFv demonstrated a slightly increased amount of HMWs compared to the F13B5 variant, which showed higher aggregation upon thermal stress (Fig. 8).

The antigen-binding activity of the stressed and unstressed samples was addressed by the antigen binding assay using SPR (Fig. 9). The analysis revealed that oxidation of scFv AK18 resulted in significantly impaired antigen-binding activity, in line with results obtained for the full length antibody. F13B5 scFv demonstrated slightly increased antigen interaction, probably due to the presence of the HMWs in the tested sample, as was shown by SEC.

Discussion

As has been demonstrated for a number of therapeutic antibodies, post-translational modifications can result in impaired stability and altered therapeutic efficacy of the molecules.[4-6,8,9,18] Oxidation of amino acids such as Met and Trp (less often Cys, His and Tyr) is one of the common modifications that can lead to loss of binding activity and alteration of the antibody Fc-receptors interactions.[8,12-14,16,17,19,52]

In this study, we examined the influence of oxidation on the functionality and stability of a novel engineered therapeutic XGFR antibody construct. Specifically, we conducted a comparative analysis of the structural and functional properties of the IGF-1R binding part of parental AK18 XGFR, which carries an oxidation-prone Trp94 residue in the CDR, and 2 of its affinity-matured variants, L31D11 and F13B5. CDR3 of L31D11 also bears Trp94, whereas F13B5 has a Tyr residue in this position. Additionally, the 3 IgG variants differ in several other amino acids involved in formation of the antigen-binding pocket (Table 1).

Comparison of the structure and function of the 3 variants demonstrated the higher antigen binding affinity of the 2 variants L31D11 and F13B5 compared to that of a parental AK18. Analysis

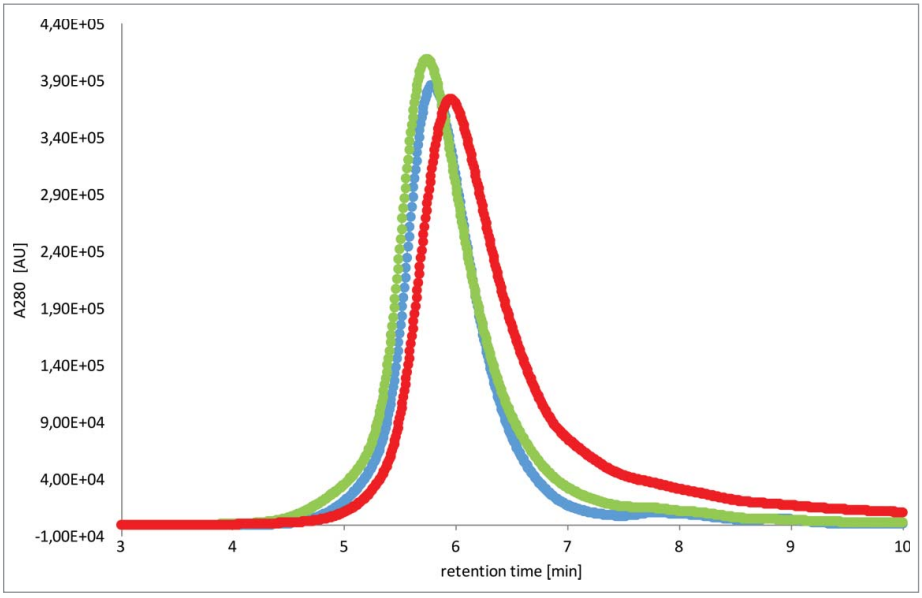

Figure 5. SEC retention profiles of purified V_L domains. AK18-V_L is shown in blue, the L31D11-V_L in red and the F13B5-V_L in green. SEC analysis was performed in PBS, pH 7.4.

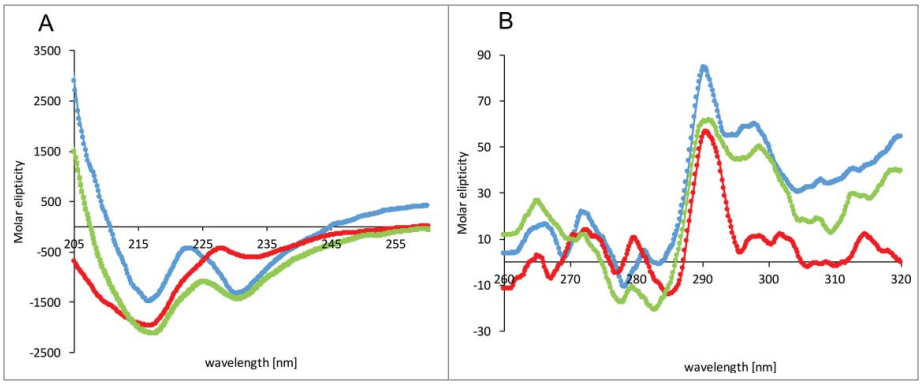

Figure 6. Spectroscopic characterization of the V_L domains. Far-UV CD spectra (A) and near-UV (B) CD spectra of the V_L domains were measured under native conditions. In the CD experiments, AK18-V_L is shown in blue, the L31D11-V_L in red and the F13B5-V_L in green.

of antibody stability revealed similar aggregation/melting temperatures for AK18 and F13B5, whereas L31D11 appeared to be less stable. When subjected to forced stress conditions, the L31D11 variant appeared to be affected by incubation at elevated temperature (in line with decreased thermal stability), and demonstrated the highest aggregation degree. In addition, MS analysis of the oxidized L31D11 antibody samples demonstrated that ~94% of the Trp94 were oxidized. Nevertheless, the binding activity of this antibody was not significantly impaired upon oxidation. On the other hand, oxidative stress applied to AK18 resulted in oxidation of 43% of Trp94, and severe antigen-binding defects (summarized in Table 6). The F13B5 antibody was not prominently affected by any of the applied stress conditions, and was the only candidate suitable for further development.

The three antibody variants studied here differed only in the composition and structure of the CDRs of the V_L domain. It has been reported previously that the solvent-exposed CDRs have a significant effect on the stability of the whole IgG.[53,54] We thus performed an extensive analysis of the respective V_L domains with regard to their structure and stability. The CD analysis of the isolated V_L domains demonstrated clear differences in secondary and tertiary structure. Moreover, the stability of the L31D11 V_L domain was lower compared to the other 2 variants. The same was true for the L31D11 scFv, and consistent with the results obtained for the full-length antibodies.

Structural modeling of the V_H domains and the respective V_L domains by the prediction tool[48] provided information about the spatial arrangement of the amino acids that are variable in the light chain CDRs of the 3 antibodies (Fig. 10A, Table 1). Interestingly, the amino acids at position 50 of the light chain (numbering according to Kabat[55]) are located in an area of the antibody paratope that is dominated by charged residues (Fig. 10B). The side chains of R91 (LC) and R98 (HC) are adding positive charges to the area surrounding position 50, which itself is variable in charge: the lysine in position 50 of the L31D11 light chain adds another positive charge to the area, whereas F13B5 is neutral in this position (Gln) and AK18 adds a negative charge (Glu). As this area is located in the center of

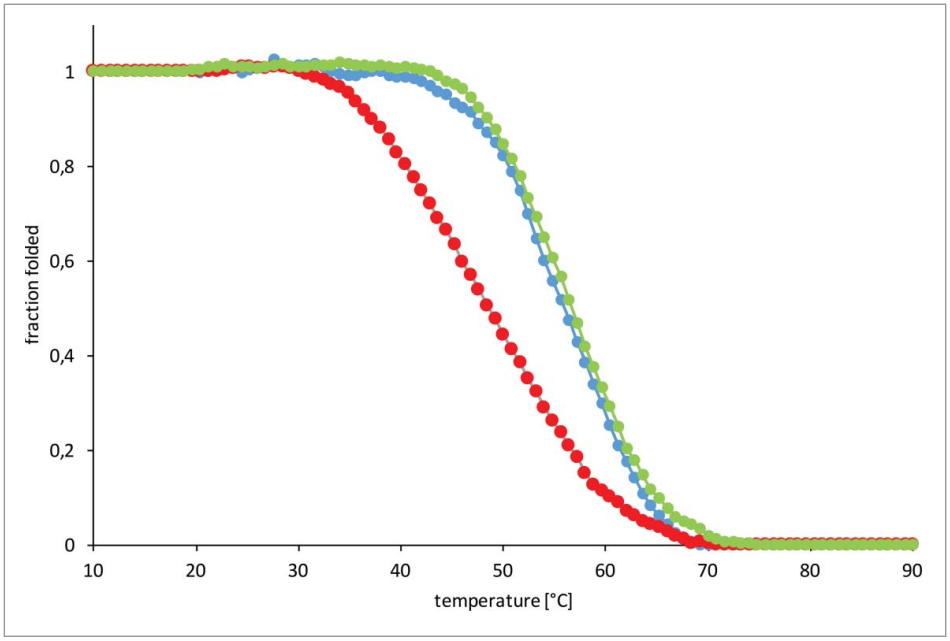

Figure 7. Thermal stability of the V_L domains of AK18, L31D11 and F13B5. Temperature induced unfolding of the V_L domains was monitored by far-UV CD spectroscopy at 218 nm. Thermal transition of AK18-V_L is shown in blue, of L31D11- V_L – in red and of F13B5- V_L – in green.

Table 5. Melting and aggregation temperatures of the test scFvs.

Sample	Tagg	Tagg_ox	Tagg 24h@40°C	Tm	Tm_ox	Tm 24h at 40°C
AK18	50.0.0	46.0	50.0	52.0	51.0	52.0
F13B5	47.0	46.0	47.0	49.0	49.0	49.0
L31D11	41.0	n/a	n/a	43.0	n/a	n/a

the paratope and close to the V_H-V_L interface, these variations in charge distribution might have an influence on target binding as well as on the stability of the molecules. L31D11, which has a lysine in position 50 and thus a repulsive character in combination with the 2 arginines in positions 91 and 98, is also the molecule with the lowest thermal stability. It should be noted that the additional positive charge of L31D11 in position 50 is partially compensated by a serine in position 53 of the light chain, but the side chains of the amino acids in position 53 are pointing away from the charged cluster formed by positions 50, 91 and 98.

In terms of antigen-binding affinity, amino acids in the CDR1 of the light chain seem to play a major role (Fig. 10C). The variable amino acids in positions 30 and 32 are exposed within the paratope, and in a good position for a productive interaction with the antigen. The highly exposed tyrosine in position 30 might be important for the high affinity of L31D11. AK18 and F13B5, which show a significantly lower affinity, carry a serine in this position, which might interact less with the antigen due to the small and less exposed side chain.

The antibody – antigen interaction is determined by amino acid residues of epitope and paratope; however, the surrounding environment of the antigen binding site also plays a critical role, e.g., by precisely defining spatial settings of the contact surfaces and providing the accurate positioning of the CDRs to assure their optimal binding configuration for the efficient antigen interaction.[56] To determine all the factors contributing to the differential binding and structure of the analyzed antibodies, and to assess all the aspects causing strongly impaired binding activity of the oxidized Trp residue in CDR of AK18 but not L31D11, more comprehensive analysis (e.g., alanine scanning mutagenesis, crystal structure) should be conducted. As the lead candidate (F13B5) has been identified, these experiments were beyond the scope of this study, and might be a subject of following investigations.

In summary, our work demonstrates that, although affinity maturation yielded IgG variants with higher affinity to antigen, one should be aware that substitution of the binding determinants in CDRs may result in altered structural features of the antibody. Thus, careful analysis with regard to both biological activity and structural properties should be performed to eliminate undesired impairment of therapeutic efficacy of the antibodies subjected to affinity maturation or designed to be devoid of critical modification-prone amino acids.

Materials and methods

Cloning, expression, and purification of the V_L domain

The pET28a plasmid encoding the V_L domains was transformed into *Escherichia coli* BL21 cells and cultivated at 37°C. At an OD600 of 0.6–0.8, protein expression was induced by addition of isopropyl β-D-1-thiogalactopyranoside (final concentration of 1 mM). Cells were harvested after overnight growth. For the inclusion body preparation, harvested cells were resuspended in inclusion body (IB) preparation buffer (100 mM TrisHCl pH 7.5, 100 mM NaCl, 1 mM ethylenediaminetetraacetic acid (EDTA)), containing inhibitor mix HP. Subsequently, the cells were disrupted and 2.5% of Triton X-100 was added; the solution was stirred for 30 min at 4°C. After centrifugation (20 min at 20000xg), inclusion bodies (IB) were washed 3 times with the IB preparation buffer. The IB pellet was solubilized and unfolded in 25 mM Tris–HCl (pH 8.0), 8 M urea, and 2 mM β-mercaptoethanol at 4°C for 4h. The soluble fraction was then injected onto a Q-Sepharose column equilibrated in 25 mM Tris–HCl (pH 8), and 5 M urea. The proteins were refolded by dialysis in 250 mM TrisHCl (pH 8.0), 100 mM NaCl, 500 mM L-Arg, 5 mM EDTA, 0.5 mM reduced glutathione and 1 mM oxidized glutathione. To remove mis-folded aggregates and remaining impurities, the

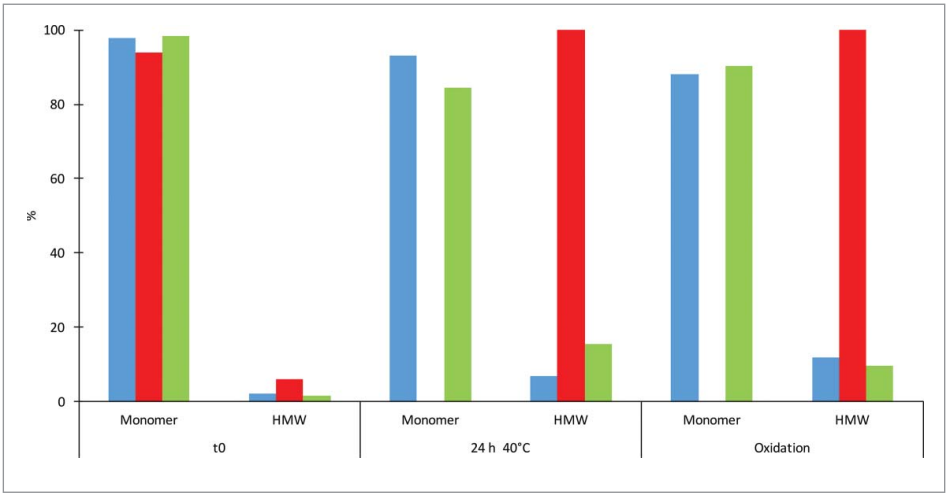

Figure 8. SEC analysis of the stress-treated scFvs of AK18 (blue), L31D11 (red) and F13B5 (green). The unstressed antibody samples (t0) were compared to samples subjected to incubation at 40°C for 24 hours and oxidation (ox).

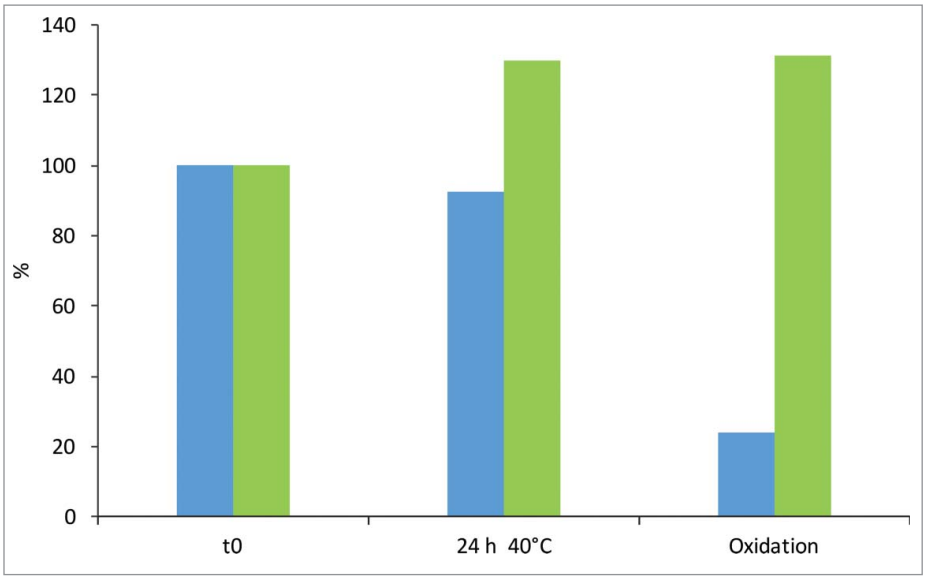

Figure 9. SPR analysis of the antigen interaction of scFvs. AK18 is shown in blue and F13B5 in green. Binding activity of the respective unstressed sample was set to 100%.

proteins were cleaned using a Superdex 75 gel-filtration column (GE Healthcare, Uppsala, Sweden) equilibrated in phosphate-buffered saline (PBS) buffer.

scFv and full-length antibodies were expressed in CHO cells. For the scFv constructs, V_L and V_H domains of the respective antibody were fused via (G4S)4 linker; in addition, C-terminal 6xHis-tag was introduced in the protein sequence. The scFvs were loaded onto the 5 ml HisTrap HP column (GE Healthcare, Uppsala, Sweden) in 20 mM Na-P, 300 mM NaCl, 10 mM imidazole, pH 7.4 and eluted with 20 mM Na-P, 300 NaCl, 500 mM imidazole pH 7.8. The protein-containing fractions were further purified using a Superdex 75 gel-filtration column (GE Healthcare, Uppsala, Sweden).

The IgGs were purified first by protein A chromatography, followed by the application of Superdex 200 gel-filtration column (GE Healthcare, Uppsala, Sweden). The recovery of intact protein was verified by matrix-assisted laser desorption/ionization time-of-flight mass spectrometry.

Preparation of the stressed samples

To achieve forced oxidation, AAPH (2,2′-azobis(2-amidinopropane) was added to protein samples in a ratio IgGs/scFvs : AAPH as 1:42. The samples were incubated light-protected in 20 mM $NH_4C_2H_3O_2$ (ammonium acetate), pH 5.0 at 40°C for 24 h.

Table 6. Influence of forced stress on the antigen binding properties of the tested antibodies.

Sample	Oxidation	Thermal stress	6x freezing / thawing
AK18			
L31D11			
F13B5			

(green - not affected, yellow - slightly reduced, red - dramatically reduced).

CD measurements

CD measurements were carried out using a Jasco J-720 spectropolarimeter (Jasco, Grossumstadt, Germany) equipped with a Peltier element. Far-UV CD spectra were measured using 10 μM protein in a 1-mm path length cuvette between 260 and 200 nm. Near-UV CD was measured between 320 and 250 nm using 50 μM protein in a 5-mm cuvette. All spectra were accumulated 16 times and buffer corrected. Thermal transitions were recorded at 218 nm with a heating and cooling rate of 20°C /h.

Analytical gel filtration

Measurements with the V_L domains were performed using a Shimadzu HPLC system (Shimadzu, Kyoto, Japan) and an analytical Superdex 75 column (GE Healthcare) equilibrated in PBS buffer. A standard flow rate of 0.75 ml/min was used. Fifty μg of V_L-samples were injected onto the column, and the elution profile was detected by fluorescence emission at 355 nm.

Analytical SEC of full-length antibodies and scFv was used to analyze aggregation propensity of the samples under different stress conditions. All experiments were carried out using Dionex Summit system with UV detection at 280 nm. Samples were analyzed with BioSuite™ 250 column in 200 mM K-Phosphate, 250 mM KCL, pH 7.0 at a flow rate 0.5 ml/min at 20°C.

Surface plasmon resonance analysis

Antigen binding assay

SPR interaction analysis was performed on a Biacore T200 system (GE Healthcare). For interaction analysis of scFv with their target, captured IgG1 glycovariants, an anti-His capturing antibody (GE Healthcare) was injected to achieve a level of 12,000 resonance units (RU). Immobilization of the capturing antibody was performed on a CM5 chip using the standard amine coupling kit (GE Healthcare) at pH 4.5. One hundred nM scFv were captured with a pulse of 60 sec at a flow rate of 10 μl/min. IGF-1R was then applied at a

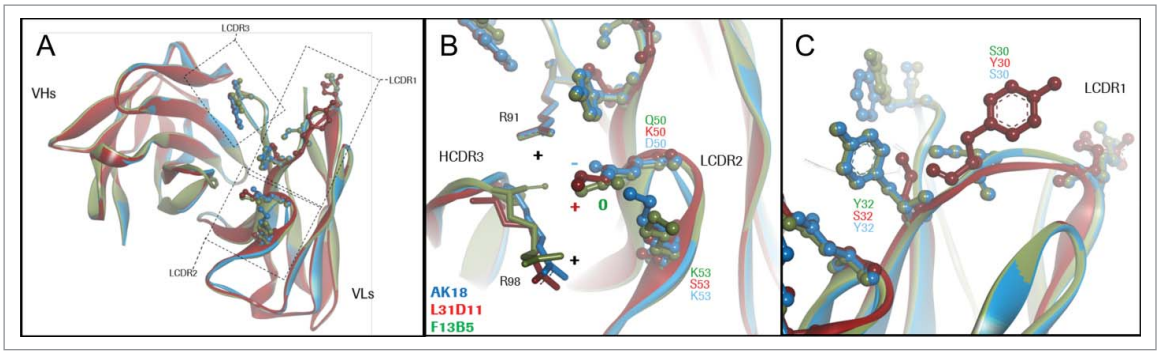

Figure 10. Homology modeling of AK18 / L31D11 / F13B5 variable domains. (A) Comparison of structural models of the 3 Fvs: AK18 (blue), L31D11 (red) and F13B5 (green). (B) Interaction of amino acid residues of LCDR2 with HCDR3. (C) Position of the solvent-exposed amino acids 30 and 32 in the CDR1 of the light chain.

concentration of 1-300 nM and a flow rate of 30 μl/min for 180 sec. The dissociation phase was monitored for 360 sec. The surface was regenerated by a 60 sec washing step with a 10 mM glycine pH 1.5 at a flow rate of 30 μl/min.

Kinetic determination

For interaction analysis of IgGs with their target, protein A (GE Healthcare) was injected to achieve a level of 5,000 resonance units (RU). Immobilization of the capturing antibody was performed on a CM5 chip using the standard amine coupling kit (GE Healthcare) at pH 4.5. Five nM test IgGs were captured with a pulse of 60 sec at a flow rate of 10 μl/min. IGF1R was then applied at a concentration of 1-300 nM and a flow rate of 30 μl/min for 120 – 180 sec. The dissociation phase was monitored for 360 sec. The surface was regenerated by a 60 sec washing step with a 10 mM glycine pH 1.5 at a flow rate of 30 μl/min.

Relative active concentration

For interaction analysis of IgGs with their target, protein A (GE Healthcare) was injected to achieve a level of 5,000 resonance units (RU). Immobilization of the capturing antibody was performed on a CM5 chip using the standard amine coupling kit (GE Healthcare) at pH 4.5. Twenty-five nM test IgGs were captured with a pulse of 60 sec at a flow rate of 5 μl/min. IGF1R was then applied at a concentration of 30 nM and a flow rate of 50 μl/min for 120 – 180 sec. The dissociation phase was monitored for 360 sec. The surface was regenerated by a 60 sec washing step with a 10 mM glycine pH 1.5 at a flow rate of 50 μl/min.

MS-analysis

Intact antibody measurements were conducted using an electron spray triple quadrupole time of flight mass spectrometer (Maxis, Bruker Corporation, Billerica, MA, USA) equipped with a Nanomate (Ithaca, NY, USA) injection system. Intact antibody data are not shown because the data are complimentary to the presented SEC data.

The oxidation levels of individual tryptophan residues were analyzed using an Orbitrap instrument (Thermo Scientific, Waltham, MA, USA), connected to an RP-UPLC (Acquity, Waters, Milford, MA, USA) via a Nanomate system. Oxidized peptide residues were identified using MASCOT MS/MS ion search (Matrix science London, UK). Quantification was achieved by selected ion monitoring through extraction of the relevant oxidized and non-oxidized peptides. The respective area counts were then used to calculate the ratio of the modified peptide.

Disclosure of potential conflicts of interest

No potential conflicts of interest were disclosed.

References

1. Reichert JM. Antibodies to watch in 2015. MAbs 2015; 7:1-8; PMID:25484055; http://dx.doi.org/10.4161/19420862.2015.988944
2. Congy-Jolivet N, Probst A, Watier H, Thibault G. Recombinant therapeutic monoclonal antibodies: mechanisms of action in relation to structural and functional duality. Crit Rev Oncol Hematol 2007; 64:226-33; PMID:17716905; http://dx.doi.org/10.1016/j.critrevonc.2007.06.013
3. Harris RJ. Heterogeneity of recombinant antibodies: linking structure to function. Dev Biol (Basel) 2005; 122:117-27; PMID:16375256
4. Harris RJ, Kabakoff B, Macchi FD, Shen FJ, Kwong M, Andya JD, Shire SJ, Bjork N, Totpal K, Chen AB. Identification of multiple sources of charge heterogeneity in a recombinant antibody. J Chromatogr B Biomed Sci Appl 2001; 752:233-45; PMID:11270864; http://dx.doi.org/10.1016/S0378-4347(00)00548-X
5. Houde D, Peng Y, Berkowitz SA, Engen JR. Post-translational modifications differentially affect IgG1 conformation and receptor binding. Mol Cell Proteomics 2010; 9:1716-28; PMID:20103567; http://dx.doi.org/10.1074/mcp.M900540-MCP200
6. Jenkins N, Murphy L, Tyther R. Post-translational modifications of recombinant proteins: significance for biopharmaceuticals. Mol Biotechnol 2008; 39:113-8; PMID:18327554; http://dx.doi.org/10.1007/s12033-008-9049-4
7. Liu H, Gaza-Bulseco G, Faldu D, Chumsae C, Sun J. Heterogeneity of monoclonal antibodies. J Pharm Sci 2008; 97:2426-47; PMID:17828757; http://dx.doi.org/10.1002/jps.21180
8. Bertolotti-Ciarlet A, Wang W, Lownes R, Pristatsky P, Fang Y, McKelvey T, Li Y, Li Y, Drummond J, Prueksaritanont T, et al. Impact of methionine oxidation on the binding of human IgG1 to Fc Rn and Fc gamma receptors. Mol Immunol 2009; 46:1878-82; PMID:19269032; http://dx.doi.org/10.1016/j.molimm.2009.02.002
9. Haberger M, Bomans K, Diepold K, Hook M, Gassner J, Schlothauer T, Zwick A, Spick C, Kepert JF, Hienz B, et al. Assessment of chemical modifications of sites in the CDRs of recombinant antibodies: Susceptibility vs. functionality of critical quality attributes. MAbs 2014; 6:327-39; PMID:24441081; http://dx.doi.org/10.4161/mabs.27876
10. Wang W, Vlasak J, Li Y, Pristatsky P, Fang Y, Pittman T, Roman J, Wang Y, Prueksaritanont T, Ionescu R. Impact of methionine oxidation in human IgG1 Fc on serum half-life of monoclonal antibodies.

Mol Immunol 2011; 48:860-6; PMID:21256596; http://dx.doi.org/10.1016/j.molimm.2010.12.009
11. Chumsae C, Gaza-Bulseco G, Sun J, Liu H. Comparison of methionine oxidation in thermal stability and chemically stressed samples of a fully human monoclonal antibody. J Chromatogr B Analyt Technol Biomed Life Sci 2007; 850:285-94; PMID:17182291; http://dx.doi.org/10.1016/j.jchromb.2006.11.050
12. Dimitrov JD, Vassilev TL, Andre S, Kaveri SV, Lacroix-Desmazes S. Functional variability of antibodies upon oxidative processes. Autoimmun Rev 2008; 7:574-8; PMID:18625447; http://dx.doi.org/10.1016/j.autrev.2008.04.009
13. Hensel M, Steurer R, Fichtl J, Elger C, Wedekind F, Petzold A, Schlothauer T, Molhoj M, Reusch D, Bulau P. Identification of potential sites for tryptophan oxidation in recombinant antibodies using tert-butylhydroperoxide and quantitative LC-MS. PLoS One 2011; 6:e17708; PMID:21390239; http://dx.doi.org/10.1371/journal.pone.0017708
14. Hu D, Qin Z, Xue B, Fink AL, Uversky VN. Effect of methionine oxidation on the structural properties, conformational stability, and aggregation of immunoglobulin light chain LEN. Biochemistry 2008; 47:8665-77; PMID:18652490; http://dx.doi.org/10.1021/bi800806d
15. Loew C, Knoblich C, Fichtl J, Alt N, Diepold K, Bulau P, Goldbach P, Adler M, Mahler HC, Grauschopf U. Analytical protein a chromatography as a quantitative tool for the screening of methionine oxidation in monoclonal antibodies. J Pharm Sci 2012; 101:4248-57; PMID: 22899501; http://dx.doi.org/10.1002/jps.23286
16. Schlothauer T, Rueger P, Stracke JO, Hertenberger H, Fingas F, Kling L, Emrich T, Drabner G, Seeber S, Auer J, et al. Analytical FcRn affinity chromatography for functional characterization of monoclonal antibodies. MAbs 2013; 5:576-86; PMID:23765230; http://dx.doi.org/10.4161/mabs.24981
17. Gao X, Ji JA, Veeravalli K, Wang YJ, Zhang T, Mcgreevy W, Zheng K, Kelley RF, Laird MW, Liu J, et al. Effect of individual Fc Methionine oxidation on FcRn binding: Met252 oxidation impairs FcRn binding more profoundly than Met428 oxidation. J Pharm Sci. 2015 Feb;104 (2):368-77; Epub 2014 Aug 29; PMID: 25175600; http://dx.doi.org/10.1002/jps.24136
18. Gaza-Bulseco G, Faldu S, Hurkmans K, Chumsae C, Liu H. Effect of methionine oxidation of a recombinant monoclonal antibody on the binding affinity to protein A and protein G. J Chromatogr B Analyt Technol Biomed Life Sci 2008; 870:55-62; PMID:18567545; http://dx.doi.org/10.1016/j.jchromb.2008.05.045
19. Liu H, Gaza-Bulseco G, Xiang T, Chumsae C. Structural effect of deglycosylation and methionine oxidation on a recombinant monoclonal antibody. Mol Immunol 2008; 45:701-8; PMID:17719636; http://dx.doi.org/10.1016/j.molimm.2007.07.012
20. Stracke J, Emrich T, Rueger P, Schlothauer T, Kling L, Knaupp A, Hertenberger H, Wolfert A, Spick C, Lau W, et al. A novel approach to investigate the effect of methionine oxidation on pharmacokinetic properties of therapeutic antibodies. MAbs 2014; 6:1229-42; PMID:25517308; http://dx.doi.org/10.4161/mabs.29601
21. Teshima G, Li MX, Danishmand R, Obi C, To R, Huang C, Kung J, Lahidji V, Freeberg J, Thorner L, et al. Separation of oxidized variants of a monoclonal antibody by anion-exchange. J Chromatogr A 2011; 1218:2091-7; PMID:21145555; http://dx.doi.org/10.1016/j.chroma.2010.10.107
22. Wei Z, Feng J, Lin HY, Mullapudi S, Bishop E, Tous GI, et al. Identification of a single tryptophan residue as critical for binding activity in a humanized monoclonal antibody against respiratory syncytial virus. Anal Chem 2007; Apr 1:79:2797-805; Epub 2014 Aug 29; PMID:17319649; http://dx.doi.org/10.1021/ac062311j
23. Boyd D, Kaschak T, Yan B. HIC resolution of an IgG1 with an oxidized Trp in a complementarity determining region. J Chromatogr B Analyt Technol Biomed Life Sci 2011; 879:955-60; PMID:21440514; http://dx.doi.org/10.1016/j.jchromb.2011.03.006
24. Peters B, Trout BL. Asparagine deamidation: pH-dependent mechanism from density functional theory. Biochemistry 2006; 45:5384-92; PMID:16618128; http://dx.doi.org/10.1021/bi052438n
25. Pace AL, Wong RL, Zhang YT, Kao YH, Wang YJ. Asparagine deamidation dependence on buffer type, pH, and temperature. J Pharm Sci 2013; 102:1712-23; PMID:23568760; http://dx.doi.org/10.1002/jps.23529
26. Zheng JY, Janis LJ. Influence of pH, buffer species, and storage temperature on physicochemical stability of a humanized monoclonal antibody LA298. Int J Pharm 2006; 308:46-51; PMID:16316730; http://dx.doi.org/10.1016/j.ijpharm.2005.10.024
27. Sinha S, Zhang L, Duan S, Williams TD, Vlasak J, Ionescu R, Topp EM. Effect of protein structure on deamidation rate in the Fc fragment of an IgG1 monoclonal antibody. Protein Sci 2009; 18:1573-84; PMID:19544580; http://dx.doi.org/10.1002/pro.173
28. Sydow JF, Lipsmeier F, Larraillet V, Hilger M, Mautz B, Molhoj M, Kuentzer J, Klostermann S, Schoch J, Voelger HR, et al. Structure-based prediction of asparagine and aspartate degradation sites in antibody variable regions. PLoS One 2014; 9:e100736; PMID:24959685; http://dx.doi.org/10.1371/journal.pone.0100736
29. Timm V, Gruber P, Wasiliu M, Lindhofer H, Chelius D. Identification and characterization of oxidation and deamidation sites in monoclonal rat/mouse hybrid antibodies. J Chromatogr B Analyt Technol Biomed Life Sci 2010; 878:777-84; PMID:20153988; http://dx.doi.org/10.1016/j.jchromb.2010.01.036
30. Yan B, Valliere-Douglass J, Brady L, Steen S, Han M, Pace D, Elliott S, Yates Z, Han Y, Balland A, et al. Analysis of post-translational modifications in recombinant monoclonal antibody IgG1 by reversed-phase liquid chromatography/mass spectrometry. J Chromatogr A 2007; 1164:153-61; PMID:17640657; http://dx.doi.org/10.1016/j.chroma.2007.06.063
31. Diepold K, Bomans K, Wiedmann M, Zimmermann B, Petzold A, Schlothauer T, Mueller R, Moritz B, Stracke JO, Mølhøj M, et al. Simultaneous assessment of Asp isomerization and Asn deamidation in recombinant antibodies by LC-MS following incubation at elevated temperatures. PLoS One 2012; 7:e30295; PMID:22272329; http://dx.doi.org/10.1371/journal.pone.0030295
32. Liu YD, van Enk JZ, Flynn GC. Human antibody Fc deamidation in vivo. Biologicals 2009; 37:313-22; PMID:19608432; http://dx.doi.org/10.1016/j.biologicals.2009.06.001
33. Vlasak J, Bussat MC, Wang S, Wagner-Rousset E, Schaefer M, Klinguer-Hamour C, Kirchmeier M, Corvaïa N, Ionescu R, Beck A. Identification and characterization of asparagine deamidation in the light chain CDR1 of a humanized IgG1 antibody. Anal Biochem 2009; 392:145-54; PMID: 19497295; http://dx.doi.org/10.1016/j.ab.2009.05.043
34. Yan B, Steen S, Hambly D, Valliere-Douglass J, Vanden BT, Smallwood S, Yates Z, Arroll T, Han Y, Gadgil H, et al. Succinimide formation at Asn 55 in the complementarity determining region of a recombinant monoclonal antibody IgG1 heavy chain. J Pharm Sci 2009; 98:3509-21; PMID:19475547; http://dx.doi.org/10.1002/jps.21655
35. Hawe A, Wiggenhorn M, van de WM, Garbe JH, Mahler HC, Jiskoot W. Forced degradation of therapeutic proteins. J Pharm Sci 2012; 101:895-913; PMID:22083792; http://dx.doi.org/10.1002/jps.22812
36. Lam XM, Yang JY, Cleland JL. Antioxidants for prevention of methionine oxidation in recombinant monoclonal antibody HER2. J Pharm Sci 1997; 86:1250-5; PMID:9383735; http://dx.doi.org/10.1021/js970143s
37. Gaza-Bulseco G, Li B, Bulseco A, Liu HC. Method to differentiate asn deamidation that occurred prior to and during sample preparation of a monoclonal antibody. Anal Chem 2008; 80:9491-8; PMID: 19072263; http://dx.doi.org/10.1021/ac801617u
38. Haverick M, Mengisen S, Shameem M, Ambrogelly A. Separation of mAbs molecular variants by analytical hydrophobic interaction chromatography HPLC: overview and applications. MAbs 2014; 6:852-8; PMID:24751784; http://dx.doi.org/10.4161/mabs.28693
39. Huang L, Lu J, Wroblewski VJ, Beals JM, Riggin RM. In vivo deamidation characterization of monoclonal antibody by LC/MS/MS. Anal Chem 2005; 77:1432-9; PMID:15732928; http://dx.doi.org/10.1021/ac0494174
40. Kang X, Kutzko JP, Hayes ML, Frey DD. Monoclonal antibody heterogeneity analysis and deamidation monitoring with high-performance cation-exchange chromatofocusing using simple, two component buffer systems. J Chromatogr A 2013; 1283:89-97; PMID:23428023; http://dx.doi.org/10.1016/j.chroma.2013.01.101
41. Kim J, Jones L, Taylor L, Kannan G, Jackson F, Lau H, Latypov RF, Bailey B. Characterization of a unique IgG1 mAb CEX profile by limited Lys-C proteolysis/CEX separation coupled with mass spectrometry and structural analysis. J Chromatogr B Analyt Technol Biomed Life Sci 2010; 878:1973-81; PMID:20554483; http://dx.doi.org/10.1016/j.jchromb.2010.05.032

42. Terashima I, Koga A, Nagai H. Identification of deamidation and isomerization sites on pharmaceutical recombinant antibody using H (2)(18)O. Anal Biochem 2007; 368:49-60; PMID:17617368; http://dx.doi.org/10.1016/j.ab.2007.05.012
43. Zhang YT, Hu J, Pace AL, Wong R, Wang YJ, Kao YH. Characterization of asparagine 330 deamidation in an Fc-fragment of IgG1 using cation exchange chromatography and peptide mapping. J Chromatogr B Analyt Technol Biomed Life Sci 2014; 965:65-71; PMID:24999246; http://dx.doi.org/10.1016/j.jchromb.2014.06.018
44. Igawa T, Tsunoda H, Kuramochi T, Sampei Z, Ishii S, Hattori K. Engineering the variable region of therapeutic IgG antibodies. MAbs 2011; 3:243-52; PMID:21406966; http://dx.doi.org/10.4161/mabs.3.3.15234
45. Nakano K, Ishiguro T, Konishi H, Tanaka M, Sugimoto M, Sugo I, Igawa T, Tsunoda H, Kinoshita Y, Habu K, et al. Generation of a humanized anti-glypican 3 antibody by CDR grafting and stability optimization. Anticancer Drugs 2010; 21:907-16; PMID:20847643; http://dx.doi.org/10.1097/CAD.0b013e32833f5d68
46. Schanzer JM, Wartha K, Moessner E, Hosse RJ, Moser S, Croasdale R, Trochanowska H, Shao C, Wang P, Shi L, et al. XGFR*, a novel affinity-matured bispecific antibody targeting IGF-1R and EGFR with combined signaling inhibition and enhanced immune activation for the treatment of pancreatic cancer. MAbs 2016; 8:811-27; PMID:26984378; http://dx.doi.org/10.1080/19420862.2016.1160989
47. Schanzer JM, Wartha K, Croasdale R, Moser S, Kunkele KP, Ries C, Scheuer W, Duerr H, Pompiati S, Pollman J, et al. A novel glycoengineered bispecific antibody format for targeted inhibition of epidermal growth factor receptor (EGFR) and insulin-like growth factor receptor type I (IGF-1R) demonstrating unique molecular properties. J Biol Chem 2014; 289:18693-706; PMID:24841203; http://dx.doi.org/10.1074/jbc.M113.528109
48. Kawanami T, Takiguchi S, Ikeda N, Funakoshi A. A humanized anti-IGF-1R monoclonal antibody (R1507) and/or metformin enhance gemcitabine-induced apoptosis in pancreatic cancer cells. Oncol Rep 2012; 27:867-72; PMID:22200743; http://dx.doi.org/10.3892/or.2011.1597
49. Gong R, Wang Y, Ying T, Feng Y, Streaker E, Prabakaran P, Dimitrov DS. N-terminal truncation of an isolated human IgG1 CH2 domain significantly increases its stability and aggregation resistance. Mol Pharm 2013; 10:2642-52; PMID:23641816; http://dx.doi.org/10.1021/mp400075f
50. Hamborg M, Kramer R, Schante CE, Agger EM, Christensen D, Jorgensen L, Foged C, Middaugh CR. The physical stability of the recombinant tuberculosis fusion antigens h1 and h56. J Pharm Sci 2013; 102:3567-78; PMID:23873630; http://dx.doi.org/10.1002/jps.23669
51. Dubnovitsky AP, Kravchuk ZI, Chumanevich AA, Cozzi A, Arosio P, Martsev SP. Expression, refolding, and ferritin-binding activity of the isolated V_L-domain of monoclonal antibody F11. Biochemistry (Mosc) 2000; 65:1011-8; PMID:11042491
52. Pan H, Chen K, Chu L, Kinderman F, Apostol I, Huang G. Methionine oxidation in human IgG2 Fc decreases binding affinities to protein A and FcRn. Protein Sci 2009; 18:424-33; PMID:19165723; http://dx.doi.org/10.1002/pro.45
53. Ionescu RM, Vlasak J, Price C, Kirchmeier M. Contribution of variable domains to the stability of humanized IgG1 monoclonal antibodies. J Pharm Sci 2008; 97:1414-26; PMID:17721938; http://dx.doi.org/10.1002/jps.21104
54. Lee CC, Perchiacca JM, Tessier PM. Toward aggregation-resistant antibodies by design. Trends Biotechnol 2013; 31:612-20; PMID:23932102; http://dx.doi.org/10.1016/j.tibtech.2013.07.002
55. Wu TT, Kabat EA. An analysis of the sequences of the variable regions of Bence Jones proteins and myeloma light chains and their implications for antibody complementarity. J Exp Med 1970; 132:211-50; PMID:5508247; http://dx.doi.org/10.1084/jem.132.2.211
56. Chi SW, Maeng CY, Kim SJ, Oh MS, Ryu CJ, Kim SJ, Han KH, Hong HJ, Ryu SE. Broadly neutralizing anti-hepatitis B virus antibody reveals a complementarity determining region H3 lid-opening mechanism. Proc Natl Acad Sci USA 2007; 104:9230-5; PMID:17517649; http://dx.doi.org/10.1073/pnas.0701279104